NIPPON STEEL & SUMITOMO METAL TECHNICAL REPORT No. 120 DECEMBER 2018

Technical Report

UDC 662 . 749 . 2 : 666 . 764 : 681 . 3

Development of Discontinuous Structure Analysis Methods and Their Applications to the Brick Structures for Coke Ovens

Kazuto YAMAMURA* Yasuyuki TAJIRI
Norio TAKEUCHI

Abstract

Brick structures that are represented by the coking chamber walls of coke ovens are subject to repeated thermal and mechanical loads in operation, and consequently cause severe damage due to brick assembly, such as joint opening, cracks and their propagation, and collapse. Numerical analysis plays a significant role in elucidating these mechanisms to predict damages and to realize optimum design of brick structure. The finite element method (FEM) is used for various problems and to produce practical results, but as it is based on continuum, it is not suited to analyzing structure consisting of many blocks, and therefore a method based on discontinuum has been developed. This paper presents an outline of the analysis technologies for brick structure using the discontinuum-based method and some applications to coke ovens.

1. Introduction

In high temperature processes such as blast furnace, coke oven, converter and secondary refining, various furnace types using shaped bricks and monolithic refractories are operated. These furnaces are subject to repetitive thermal and mechanical loads under operation, and various types of deterioration and/or damage are caused. In a furnace such as the coke oven of brick structure in particular, multi-stage fractures take place, where the fractures start at the deformation and/or the crack generated in the early stage, and reach collapse in the final stage via the minor-scale fractures in the middle stage. Namely, it is the phenomenon of the generation of deformation and crack due to joint opening that specifically takes place in the contact aggregate of a number of blocks, and the evolution thereof to collapse.

Elucidation of the mechanism of the phenomenon to predict and prevent damages and to prolong the furnace life is required. In order to realize the function matching the operation and prolonged furnace life, optimizations of the brick structure (material, shape, joint, dowel, and so forth) and the brick assembly structure are required. Numerical structural analysis plays a significant role in these effects, and the finite element method (FEM) is utilized as a powerful tool. However, because FEM is a continuum-based analysis method, it is inappropriate for the structural analysis of the aggregate consisting of a number of contacting bodies; therefore, to date, a number of discontinuum-based analysis methods have been developed, and put into practical use. On the other hand, in the actual fields of operation and designing, not the behavior after fracture but grasping the state of limit (deformation and/or stress) just before fracture is important. Therefore, in order to predict the ultimate strength, the development and the application to practical use of the discrete limit analysis method that considers elements as rigid have been promoted. Following on from that, from the needs of evaluating the stiffness and the strength of the furnace wall including those in the initial stage of operation, the development of new analysis methods dealing with the deformation of the rigid elements was started and has been continued up to the present day.

In this article, the outline of the approach to the analysis of the brick structure by using the discontinuous structure analysis method, and the application to various problems of the coke oven are introduced.

2. Discontinuous Structure Numerical Analysis Method and Applicability to Brick Structure

2.1 FEM for continuum

FEM is the most popular and important numerical analysis method at present, and is widely used for various issues including

* Chief Researcher, Process Technology Div., Process Research Laboratories
20-1 Shintomi, Futtsu City, Chiba Pref. 293-8511

highly sophisticated nonlinear problems. From a historical viewpoint, the process has been developed based on the displacement method by using displacement as an unknown quantity. However, although the continuity of the displacement on a boundary surface among elements is maintained, and the accuracy of the displacement analysis is high, the continuity of the surface force on the boundary surface is not guaranteed. Therefore, the method is inappropriate to deal with the discontinuous state such as exfoliation and/or slipping (so-called contact problem). In order to solve this problem, various methods (link element method[1] and joint element method[2]) have been developed. However, even today, the analysis of the state of large-scale multibody contact such as brick structures is substantially difficult.

Regarding this problem, pseudo presentation of the behavior has been attempted, for instance by using a quantity of Young's modulus much smaller than that of the brick for the joint material and/or by incorporating nonlinearity into the joint behavior. However, these attempts resulted in generating problems such as unnatural tensile stress and/or poor calculation convergence.

On the other hand, the usability of FEM is high for the detailed thermal stress analysis of a single brick and/or minor-scale system consisting of several bricks, and used separately from the discontinuous structure analysis method.

2.2 Rigid body spring model (RBSM) for discontinuum

As a means to investigate the criteria of fracture in the introduction, Nippon Steel & Sumitomo Metal Corporation focused its attention on the discrete limit analysis method and RBSM[3] developed by Kawai. The company developed the brick structure analysis tool (NS-Brick)[4, 5] by incorporating into the model the thermal stress analysis function and a joint model specific to brick structures.

This method is based on Kawai's concept that "the essence of deformation and/or fracture resides in slipping". In the method, elements are assumed as rigid body, and springs are assumed in the directions of the normal and the tangential direction respectively on the boundary surface between elements, and the surface force between elements is calculated based on the relative displacement between the elements. This method deals with the surface force that cannot be handled by FEM, and with this spring, the energy corresponding to the element deformation is evaluated, and the stiffness equation is solved.

This method is also capable of handling the fracture in progress to final collapse by evaluating the exfoliation and/or the slip on the boundary surface. The load leading to the final collapse gives an upper limit value; therefore, discrete limit analysis is possible. Furthermore, as this method has no nodal points, the element shape can be determined arbitrarily. However, as the element is rigid and the state of the inside of the element is unknown, the prediction of the interim state of the fracture of the brick structure ongoing to the final collapse is confined to actions such as displacement and/or partial fracture.

The NS-Brick that employs RBSM realizes the limit analysis effectively with a lower degree of freedom, and is usable in that it can evaluate the final strength of the brick structure without asking for the accuracy in displacement, and had been applied to actual problems until HPM in the next section was introduced.[6, 7]

2.3 Hybrid-type penalty method (HPM) for discontinuum

If the element internal deformation such as the one dealt with by FEM, and the surface force on the element boundary surface or its equivalent are dealt with simultaneously, the progress of fracture can be calculated consistently from the minute deformation level to collapse. Then, by slightly weakening the continuity of the displacement on the element boundary surface, and by changing the collateral condition pertaining to the continuity of displacement to variational presentation by using the Lagrange multiplier, the said multiplier becomes equal to the surface force on the element boundary surface, and further, the field of displacement can be assumed independently. Takeuchi et al. focused their attention on the hybrid-type variational model[8, 9], and developed HPM[10, 11] by introducing the concept of spring to the Lagrange multiplier. Further, they developed the new brick structure analysis tool (NS-Brick II) equipped with the thermal stress analysis function[12] and the joint model for intensification to be able to cope with various nonlinearities.

In this method, the analysis region is divided into minute partial regions, an independent displacement field is assumed in each partial region, and the continuity of the displacement is approximated by the penalty. Because the Lagrange multiplier denotes the surface force, the analysis of progressive type fractures is possible like RBSM. Furthermore, if a linear displacement field using the rigid-body displacement (parallel displacement and rigid body rotation) and the strain at an arbitral point in a partial region is applied to each partial region, the accuracy of the elastic solution of HPM becomes equal to that of the constant strain element in FEM, and the discrete limit analysis can be executed, while maintaining the accuracy of the elasticity solution.

In HPM, as the continuity of the surface force and the collapse mechanism are secured, the method gives the upper bound side collapse load for the true solution similarly to RBSM. The collapse load on the lower bound side can be found for the true solution by taking into consideration the plastic condition in the partial region. Namely, pinching of the limit load with upper and lower bound solutions so far difficult to realize becomes possible.[13]

NS-Brick II using HPM realizes the evaluation in a wide range from the brick deformation (stiffness) to the final strength consistently, and is applied to practical problems as a principal means in a wide range, taking the place of RBSM.[7, 14]

2.4 Other methods of discontinuum analysis

The discontinuum analysis methods are basically divided into two types: the continuum-based type and the discontinuum-based type. The former is represented by FEM, which deals with the discontinuum with the addition of the contact analysis function. The latter is further divided into two types, depending on whether they handle a phenomenon statically or dynamically. RBSM and HPM discussed in this article belong to the statically handled category. Further to this recently, the study on the meshfree discrete limit analysis method[15] based on the unified energy principle by Kawai[15] is in progress, and evolution to a highly accurate solution of contact problems is expected.

Regarding the methods that belong to the dynamically handled category, there is the distinct element method (DEM) of Cundall[16] in which the element is assumed as a rigid body and the elements are connected with a spring and a dashpot, and the equation of motion established in each element is solved successively by difference calculus,[16] and the discontinuous deformation analysis (DDA) of Shi et al.[17] in which the contact, slip, collision and the separation between blocks are handled dynamically. This method is formulated, taking into consideration the strain in addition to the rigid-body displacement and the rigid-body rotation of the block. The application of the method to stone fall analysis and/or base rock fall analysis is under way. It can also be easily applied to the refractory structure. In addition to DDA, the manifold method is available.[18]

Furthermore, in company with the progress of computers, the particle method has also made remarkable progress. There are two types of particle method, the method to describe a continuum as the aggregate of particles, and the other method to solve the mechanical contact dynamically by considering a particle as a rigid body. The former is represented by the smoothed particle hydro-dynamics (SPH) of Lucy et al.[19], and the moving particle semi-implicit (MPS) of Koshizuka et al.[20] In these methods, a continuum is considered as the aggregate of movable particles, wherein, by calculating the smoothened physical quantities successively with a weighting function, and solving the governing equations pertaining to each particle successively, the position of each particle is renewed. The latter is represented by the aforementioned DEM. The particle method has been developed as a method for fluid analysis, and judging from its original function, the application to discontinuum can be made with relative ease, and recently, it has been used for structural bodies.[21, 22)]

Furthermore, methods composed of the linkage of the above-mentioned various methods have been proposed, and have been put into practical use. For instance, they are the combinations of FEM and DEM, and SPH and DEM. Additionally, there is another method, the particle finite element method (PFEM)[23], in which the nodal point of FEM is considered as a particle and dealt with in a Lagrange-like manner, and FEM computation is conducted in succession by applying remesh. The application of these dynamic solution methods remains a subject for future study.

3. Formulation of Structure Analysis Method of Brick Structure

3.1 HPM

3.1.1 Hybrid-type variation principle

(1) Fundamental equation of elasticity problem

An elastic stress field Ω having a boundary Γ as shown in **Fig. 1** is considered. The fundamental equation in Ω is represented as follows.

Equilibrium equation

$$\mathrm{div}\boldsymbol{\sigma} + \mathbf{f} = 0 \quad \text{in } \Omega \tag{1}$$

Constitutive equation

$$\boldsymbol{\sigma} = \mathbf{D} : \boldsymbol{\varepsilon} \tag{2}$$

Strain-displacement relational equation

$$\boldsymbol{\varepsilon} = \nabla^s \mathbf{u} = \frac{1}{2}\{\nabla\mathbf{u} + {}^t(\nabla\mathbf{u})\} \tag{3}$$

Where, $\mathbf{u}$: displacement field in Ω, $\boldsymbol{\varepsilon}$: strain, $\boldsymbol{\sigma}$: stress, $\mathbf{D}$: elastic tensor and $\mathbf{f}$: body force. When it is assumed that Γ_u is the geometrical boundary given by displacement $\hat{\boldsymbol{u}}$, and Γ_σ is the kinetic boundary given by the surface force $\hat{\boldsymbol{t}}$, they satisfy the following conditions.

Geometrical boundary condition

$$\boldsymbol{u}|_{\Gamma_u} = \hat{\boldsymbol{u}} \quad \text{(given)} \tag{4}$$

Mechanical boundary condition

$$\boldsymbol{\sigma}|_{\Gamma_\sigma}\hat{\boldsymbol{n}} = \hat{\boldsymbol{t}} \quad \text{(given)} \tag{5}$$

Where, $\boldsymbol{t}$: surface force, $\boldsymbol{n}$: normal vector in the outward direction on the boundary and $\boldsymbol{t} = \boldsymbol{n\sigma}$.

(2) Hybrid-type virtual work principle

The following virtual work equation is obtained by multiplying Eq. (1) with the virtual displacement $\delta\boldsymbol{u}$ that satisfies the geometrical boundary condition, then applying volume integration with respect to region Ω, applying the Gauss divergence theorem and rearranging.

$$\int_\Omega \boldsymbol{\sigma} : \mathrm{grand}\,\delta\boldsymbol{u}dV - \int_\Omega \boldsymbol{f}\cdot\delta\boldsymbol{u}dV - \int_{\Gamma_\sigma}\hat{\boldsymbol{t}}\cdot\delta\boldsymbol{u}dS = 0 \tag{6}$$

The region Ω is, as shown in **Fig. 2**, assumed to consist of the division of partial region $\Omega^{(e)}$ which is surrounded by the closed boundary $\Gamma^{(e)}$ of M in total number, then Eq. (6) is expressed as follows as the summation of each partial region.

$$\sum_{e=1}^{M}\left(\int_{\Omega^{(e)}}\boldsymbol{\sigma} : \mathrm{grand}\,\delta\boldsymbol{u}dV - \int_{\Omega^{(e)}}\boldsymbol{f}\cdot\delta\boldsymbol{u}dV - \int_{\Gamma^{(e)}}\boldsymbol{t}\cdot\delta\boldsymbol{u}dS\right) = 0 \tag{7}$$

When the displacement on the common boundary $\Gamma_{\langle ab\rangle}$ of the two adjoining partial regions of $\Omega^{(a)}$ and $\Omega^{(b)}$ is denoted as $\tilde{\boldsymbol{u}}^{(a)}$ and $\tilde{\boldsymbol{u}}^{(b)}$, the following equation is arranged.

$$\tilde{\boldsymbol{u}}^{(a)} = \tilde{\boldsymbol{u}}^{(b)} \quad \text{on } \Gamma_{\langle ab\rangle} \tag{8}$$

This collateral condition is expressed as the following by using the Lagrange multiplier λ.

$$H_{ab} \overset{\mathrm{def}}{=} \delta\int_{\Gamma_{\langle ab\rangle}}\lambda\,(\tilde{\boldsymbol{u}}^{(a)} - \tilde{\boldsymbol{u}}^{(b)})\,dS \tag{9}$$

By inserting this collateral condition into the virtual work of Eq. (7), and further by considering the thermal stress $\boldsymbol{\sigma}_T$, the hybrid-type virtual work equation becomes the following. The number of the adjoining element boundary sides is N.

$$\sum_{e=1}^{M}\left(\int_{\Omega^{(e)}}\boldsymbol{\sigma} : \mathrm{grand}\,\delta\boldsymbol{u}dV - \int_{\Omega^{(e)}}\boldsymbol{\sigma}_T : \mathrm{grand}\,\delta\boldsymbol{u}dV - \int_{\Omega^{(e)}}\boldsymbol{f}\cdot\delta\boldsymbol{u}dV - \int_{\Gamma^{(e)}}\boldsymbol{t}\cdot\delta\boldsymbol{u}dS\right)$$
$$-\sum_{s=1}^{N}\left(\delta\int_{\Gamma_{\langle s\rangle}}\lambda\,(\tilde{\boldsymbol{u}}^{(a)} - \tilde{\boldsymbol{u}}^{(b)})\,dS\right) = 0 \tag{10}$$

When $\boldsymbol{t}^{(a)}$ and $\boldsymbol{t}^{(b)}$ are considered as the surface forces on the boundary $\Gamma_{\langle ab\rangle}$, the following equation is arranged, where the Lagrange multiplier λ denotes the surface forces on $\Gamma_{\langle ab\rangle}$.[9]

$$\lambda = \boldsymbol{t}^{(a)} = -\boldsymbol{t}^{(b)} \tag{11}$$

3.1.2 Discretized equation of HPM

(1) Displacement field independent in each partial region

Displacement field $\boldsymbol{u}^{(e)}$ is considered as independent in the respective partial region (e), and assumed as the following.

$$\boldsymbol{u}^{(e)} = \boldsymbol{N}_d^{(e)}\boldsymbol{d}^{(e)} + \boldsymbol{N}_\varepsilon^{(e)}\boldsymbol{\varepsilon}^{(e)} \tag{12}$$

Where, $\boldsymbol{d}^{(e)}$: displacement and rotation of a rigid body in a partial region, $\boldsymbol{\varepsilon}^{(e)}$: a constant strain in the partial element, $\boldsymbol{N}_d^{(e)}$, $\boldsymbol{N}_\varepsilon^{(e)}$: coefficient matrix and is the function of the coordinate. As Eq. (12) shows, because the displacement field is expressed by the rigid body displacement and the rigid body rotation with the degree of freedom of strain and its gradient, and differently from the displacement method FEM, it does not share the displacement at the apex or the nodal point, and is not governed by shape function. Accordingly, the element shape is not particularly confined, and any shapes of polygons, polyhedrons and/or curved face bodies can be used as the partial region.

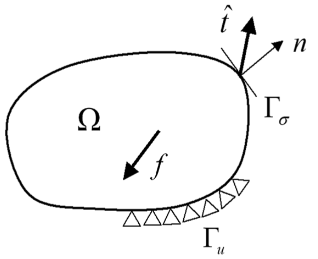

Fig. 1 Elastic stress field

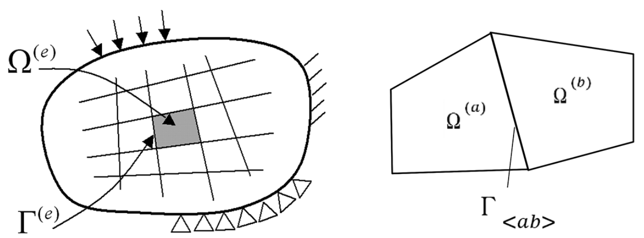

Fig. 2 Partial region and boundary

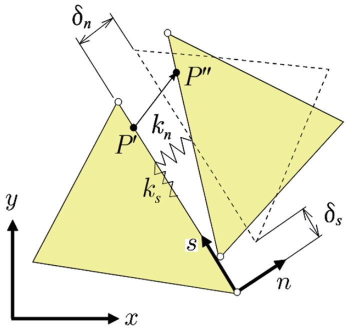

Fig. 3 Relation between *k* and $\delta_{<ab>}$

(2) Lagrange multiplier and penalty

As shown by Eq. (11), as the Lagrange multiplier λ on the boundary of $\Gamma_{<ab>}$ physically denotes the surface force, λ is redefined with the spring stiffness (penalty function) and the relative displacement on the boundary as below.

$$\lambda_{<ab>} = k \cdot \delta_{<ab>} \tag{13}$$

Where, $\delta_{<ab>}$: relative displacement on the element boundary $\Gamma_{<ab>}$, and k: matrix correlating the surface force and the relative displacement.

In the case of the three-dimensional problem, λ is assumed as below.

$$\begin{Bmatrix} \lambda_{n<ab>} \\ \lambda_{s<ab>} \\ \lambda_{t<ab>} \end{Bmatrix} = \begin{bmatrix} k_s & 0 & 0 \\ 0 & k_t & 0 \\ 0 & 0 & k_n \end{bmatrix} \begin{Bmatrix} \delta_s \\ \delta_t \\ \delta_n \end{Bmatrix} \tag{14}$$

As **Fig. 3** shows, in the case of the two-dimensional problem, $\delta_{n<ab>}$ and $\delta_{s<ab>}$ are the relative displacements in the normal direction and in the tangential direction from the element boundary $\Gamma_{<ab>}$, and similarly, $\lambda_{n<ab>}$ and $\lambda_{s<ab>}$ are the Lagrange multipliers λ in the normal direction and in the tangential direction, or the surface force.

By inserting Eq. (12) and (13) into Eq. (10), the discretized equation of HPM is obtained as below (derivation process omitted).

$$\begin{aligned} &\mathbf{KU} = \mathbf{P} \\ &\mathbf{K} = \sum_{e=1}^{M} \mathbf{K}^{(e)} + \sum_{s=1}^{N} \mathbf{K}_{<s>} \\ &\mathbf{P} = \sum_{e=1}^{M} \mathbf{P}^{(e)} + \sum_{e=1}^{M} \mathbf{P}_T^{(e)} \end{aligned} \tag{15}$$

Where, $\mathbf{U}$: displacement vector of entire system, $\mathbf{P}^{(e)}$: load term, $\mathbf{P}_T^{(e)}$: thermal load term, $\mathbf{K}_{<s>}$: coefficient matrix pertaining to collateral condition, and $\mathbf{K}^{(e)}$: term pertaining to stiffness of element.

In the case of HPM, $\mathbf{U}$ is expressed as $\mathbf{U} = \lfloor \boldsymbol{d}, \boldsymbol{\varepsilon} \rfloor^t$ with rigid-body displacement $\boldsymbol{d}$ and strain $\boldsymbol{\varepsilon}$, which becomes the following when the element area is expressed as $\mathbf{A}^{(e)}$ and the constituent matrix as $\mathbf{D}^{(e)}$.

$$\mathbf{K}^{(e)}\mathbf{U}^{(e)} = \begin{bmatrix} 0 & 0 \\ 0 & \mathbf{A}^{(e)}\mathbf{D}^{(e)} \end{bmatrix} \begin{Bmatrix} \boldsymbol{d}^{(e)} \\ \boldsymbol{\varepsilon}^{(e)} \end{Bmatrix} \tag{16}$$

By using the relation of Eq. (16), the discretized equation of Eq. (15) is expressed as follows in more detail.

$$\begin{bmatrix} \mathbf{K}_{dd} & \mathbf{K}_{d\varepsilon} \\ \mathbf{K}_{\varepsilon d} & \mathbf{K}_{\varepsilon\varepsilon} + \mathbf{D} \end{bmatrix} \begin{Bmatrix} \boldsymbol{d} \\ \boldsymbol{\varepsilon} \end{Bmatrix} = \begin{Bmatrix} \mathbf{P}_d \\ \mathbf{P}_\varepsilon \end{Bmatrix} \tag{17}$$

Thus the discretized equation (17) consists of a term generated by the collateral condition and a term generated by the element stiffness.

3.2 Discretized equation of RBSM[24–27]

In RBSM, as opposed to the linear displacement field of Eq. (12), the following rigid-body displacement field is assumed.

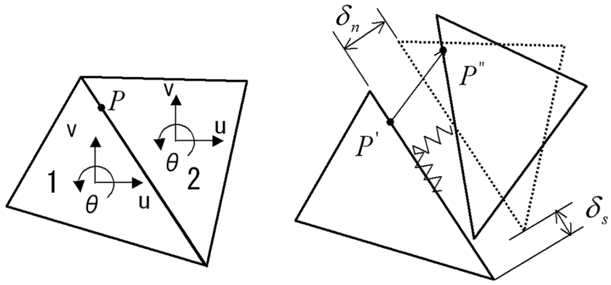

Fig. 4 Rigid body and spring system in RBSM

$$\boldsymbol{u}^{(e)} = \boldsymbol{N}_d^{(e)} \boldsymbol{d}^{(e)} \tag{18}$$

With the application of this relation to the evolution of HPM, Eq. (17) is expressed as follows.

$$\mathbf{K}_{dd}\boldsymbol{d} = \mathbf{P}_d \tag{19}$$

Where, the coefficient matrix is as follows.

$$k_{dd}^{<ab>} = \int_{\Gamma_{<ab>}} {}^t\boldsymbol{N}_d^{(a)} k \boldsymbol{N}_d^{(b)} d\Gamma \tag{20}$$

In HPM, k of Eq. (20) denotes the penalty function assumed in Eq. (13). In the meantime, in RBSM, as **Fig. 4** shows, k is considered as a spring constant and assumed as the following.

$$\begin{Bmatrix} \lambda_n \\ \lambda_s \end{Bmatrix} = \begin{bmatrix} k_n & 0 \\ 0 & k_s \end{bmatrix} \begin{Bmatrix} \delta_n \\ \delta_s \end{Bmatrix} \tag{21}$$

With the use of this spring constant, Eq. (17) agrees with the discretized equation of RBSM.

3.3 HPM material nonlinear analysis by load increment method

One of the analysis methods for material nonlinear problems is the load increment method based on the r_{min} method.[28] In HPM, this method was extended so as to be applied to the problems accompanying destressing, and is applied to the nonlinear analysis which can also easily deal with the fracture in partial regions.[29]

As a fracture standard, the method is applied to slip (Mohr-Coulomb condition, Mises condition) (unloading), tension crack (recontact), shearing crack and the nonlinear joint (to be discussed later).

3.4 Definition of nonlinear joint for brick structure analysis

In HPM, the penalty function is used for the spring constant. Various joint functions specific to brick structures are defined in the penalty function, and the brick structure analysis is made possible. The list of the nonlinear joint specifications presently introduced to HPM is shown in **Table 1**.

4. Applications to the Coke Oven

4.1 Brick structures of coking chamber wall and damage[30–32]

Many of the coke ovens in Japan have been operated for longer than forty years, and the deterioration of furnace structure has progressed due to the long-term operation, and thus the problem of deterioration of production capacity and energy efficiency has emerged. However, repairing of coke ovens requires an extended work period and high cost, and the demand for prolonged service life and the highly durable wall structures of existing coke ovens is strong.

Although the brick walls of carbonization chambers are built of silica bricks excellent in stability for thermal volumetric change, they suffer from the yearly increase of damages caused by the repetitive thermal and mechanical loads exerted in the daily operations of charging coal and discharging coke.

Figure 5 shows a diagram depicting a coke oven and the typical damage patterns of chamber walls. The types of damages to the chamber walls are: spalling of bricks in the neighborhood of the car-

Table 1 List of nonlinear joint

Classification	Joint mechanism	Initial thickness	Strength
Simple joint			
① Dry joint	Simple contact	Zero	•TS: Zero •CS: ∞
② Initial gap	Thermal expansion allowance	Non zero	•TS: Zero •CS: ∞ (after contact)
Joint materials			
③ Unshaped refractories (mortar etc.)	Bonding	Non zero	•TS: Non zero •Compressibility
④ Cushion material (blanket etc.)	Thermal expansion allowance	Non zero	•TS: Zero •Compressibility
⑤ Another special material (styrofoam etc.)	Dissipation after operation	Non zero	•TS: Zero •Compressibility
Changing of joint status after operation			
⑥ Entry of foreign matter into joint (carbon etc.)	Latchet deformation	Zero or non zero	•TS: Zero •CS: ∞
⑦ Generation of gap	Shrinkage by drying	Zero Initialized to zero	•TS: Zero •CS: ∞ (after contact)

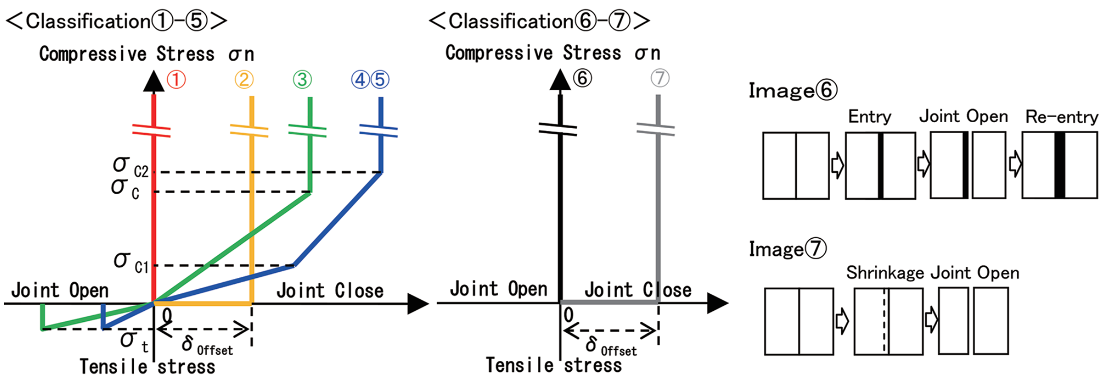

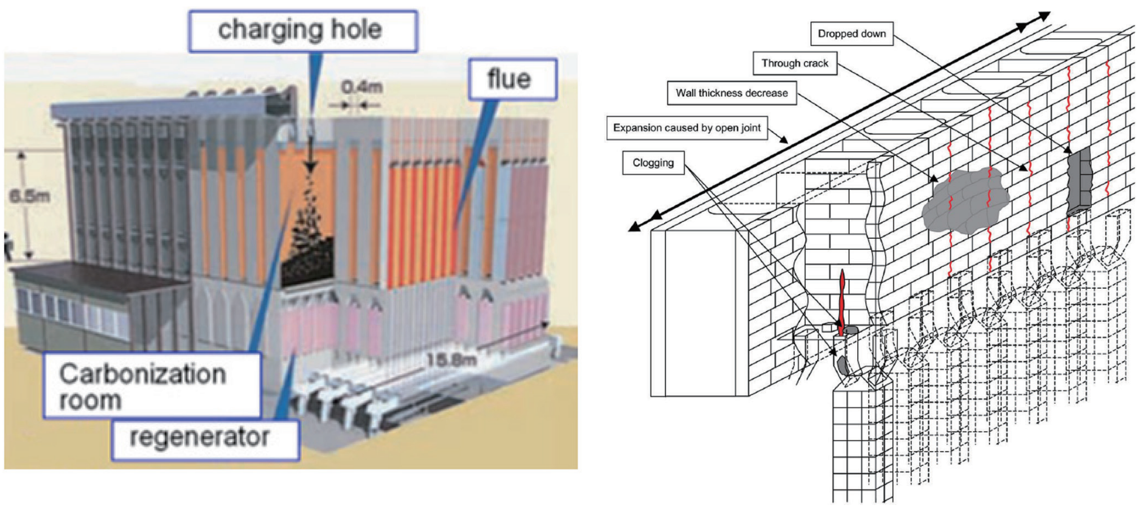

Fig. 5 Coke oven and typical damage patterns of chamber wall[32)]

bonization chamber mouth, yearly developed wear of bricks, wall thickness decrease caused by the separation of the carbon which had once adhered to the wall bricks through cracks generated at nearly equal intervals in the furnace direction, growth thereof and the deterioration of the wall stiffness, expansion of the furnace due to the penetration of carbon into the opening of the joint and cracks, and corner break of the brick in the neighborhood of the horizontal joint near the furnace bottom. As a result of the interactive effects and/or the vicious circle of the abovementioned damages, the deterioration of the furnace wall bearing force, the generation of through holes and/or the collapse of the wall are considered.

In this section, the influence of the brick structure type on the wall stiffness and the strength, and the results of the analysis on the cause of the through cracks and the through holes of the chamber walls are introduced.

4.2 Subject brick structure for study

Figure 6 shows the basic unit structure of the brick structure studied in this article, of which (a) is termed as Type I and (b) as Type II. The upper and the lower bricks that run horizontally are the carbonization chamber bricks (hammer brick and laufer brick), and constitute a combustion space with the binder bricks that connect the upper and the lower carbonization chamber bricks. In the actual furnace, there are about 20 unit structures of either of these types in the furnace length direction (crosswise direction on the figure), and about several tens of it in the vertical direction (in the direction perpendicular to the figure).

4.3 Stiffness and strength of chamber wall

4.3.1 Objective of analysis

The objectives of the analysis are to: evaluate the stiffness and the strength of the basic block and the wall which is the aggregation of the basic blocks, confirm the validity of the analysis method, and grasp the fundamental properties of the brick structure. This analysis mainly deals with the changes in deformation and the state of stress when a mechanical load is exerted, in which thermal stresses are out of scope.

4.3.2 Subject of analysis and model

(1) Subject of analysis: brick structures of the types shown in Fig. 6.

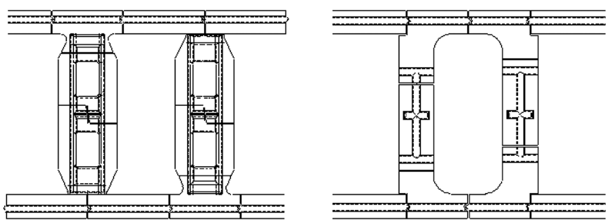

(a) Type I (b) Type II

Fig. 6 Types of brick structures

(2) Region of modelling: basic blocks of 5 steps with two binders, and the wall of 50 steps with 10 binders (1/2 symmetrical model), dowel and joint are taken into consideration.
(3) Mesh: models of basic block and wall as shown in **Fig. 7**.
(4) Material properties: shown in **Table 2**.
(5) Heat transfer conditions: behavior of the subject under the effect of mechanical load is evaluated and the effect of temperature distribution is out of scope.
(6) Loading conditions: shown in **Fig. 8**. Concentrated load that affects through holes is applied to the basic block, and the coal carbonization pressure during operation is applied to the wall

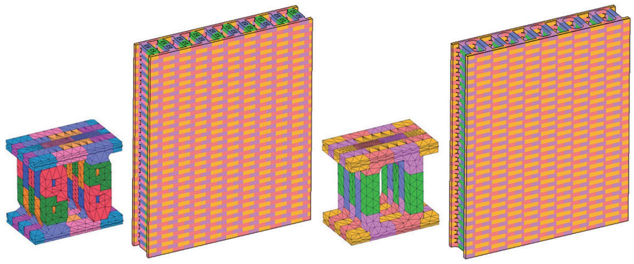

(a) Type I (b) Type II

Fig. 7 Types of brick structure and models

Table 2 Material properties

Property	Unit	Brick	Joint
Young’s modulus	GPa	12.0	0.03
Poisson’s ratio	—	0.25	0.25
Tensile strength	MPa	5.0	0.1
Compressive strength	MPa	50.0	5.0
Shear strength	MPa	10.0	10.0
Internal friction angle	°	65.0	65.0
Thermal conductivity	1/°C	1.0E-5	1.0E-5
Heat transfer coef.	W/mK	0.77	0.77
Specific heat	kcal/kgK	0.17	0.17
Density	kg/mm^3	1.8E-6	1.8E-6

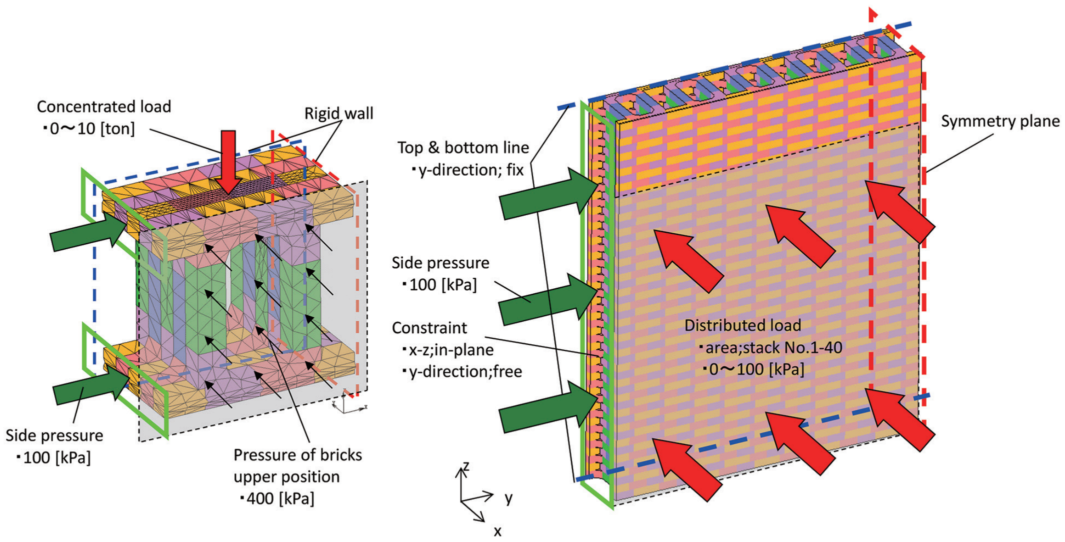

(a) Basic block model (b) Wall model

Fig. 8 Loading & boundary conditions (Type II)

with the addition of the furnace shrinking load (side pressure) and the brick weight in the furnace height direction from the top (pressure exerted by bricks in the upper position).

(7) Boundary condition: shown in Fig. 8. Symmetrical across the periphery.

4.3.3 Analysis method

(1) Method: NS-Brick II (HPM)

(2) Type of analysis: Elastic analysis

(3) Type of element: Tetrahedral element

4.3.4 Analysis case

In this study, analyses pertaining to the types of brick structures of Type I and Type II for the cases of the basic block structure and the wall structure under the single loading condition as shown in Fig. 8 were conducted. **Table 3** shows the cases of this analysis.

4.3.5 Analysis result

(1) Stiffness and strength of the basic block

Figures 9 and **10** show the deformation of the basic blocks under the maximum load (magnitude: ×10) and the displacement-load curve at the loading point, respectively. From this analysis result, the following tendencies were revealed. Because the HPM computation terminates when the judgement of collapse such as the secession of elements is made numerically, this article confines its evaluations to the stiffness in the early stage (in the elasticity region mainly) and the strength (inflection point of the displacement-load curve).

(i) The block stiffness (= load divided by displacement at the loading point) of Type I in the early stage is almost equal to that of Type II.

(ii) The strength denoted by the inflection point of the displacement-load curve (shown with ○ in Fig. 10) of Type I is higher than that of Type II.

(iii) Cracks generated by the bending stress are observed on the combustion side of the laufer section in Type I (shown with ○ in Fig. 9).

(2) Stiffness and strength of wall

Figures 11 and **12** show the deformation of the wall under the maximum load (magnitude: ×30) and the displacement-load curve at the loading point, respectively. This analysis result revealed the following tendencies.

(i) In Type I, the largest joint opening is generated at the position in the area between the 28th step to 33rd step which is slightly above the center of the wall in the height direction (at the 25th step).

(ii) The wall stiffness of Type II (= load divided by the displacement at the loading point) in the early stage is higher than that of Type I.

(iii) The strength of Type II denoted by the inflection point of the

Table 3 Analysis cases

Case		Type	Region of modeling
Basic block	Case-S1	Type I	5 layers × 2 bindars
	Case-S2	Type II	5 layers × 2 bindars
Wall	Case-W1	Type I	50 layers × 10 bindars
	Case-W2	Type II	50 layers × 10 bindars

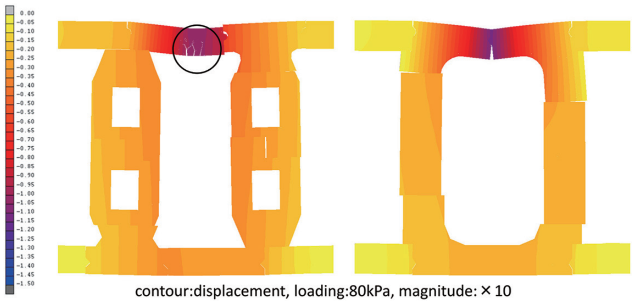

(a) Type I (b) Type II

Fig. 9 Deformation of the basic blocks

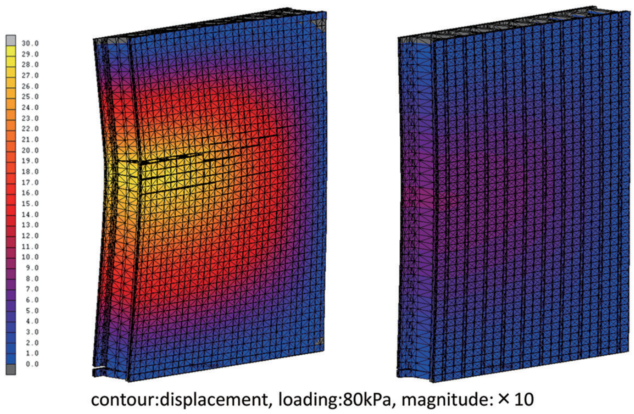

(a) Type I (b) Type II

Fig. 11 Deformation of the wall

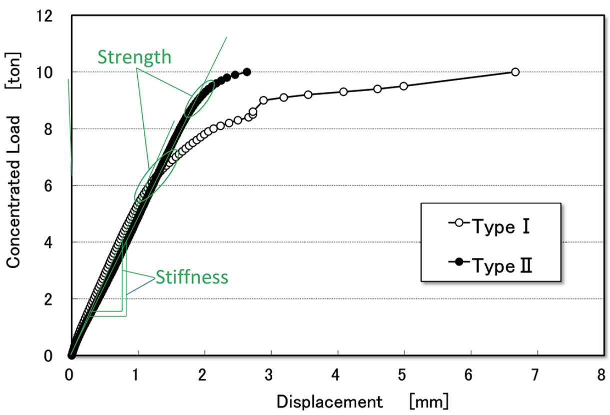

Fig. 10 Strength and stiffness of the basic blocks

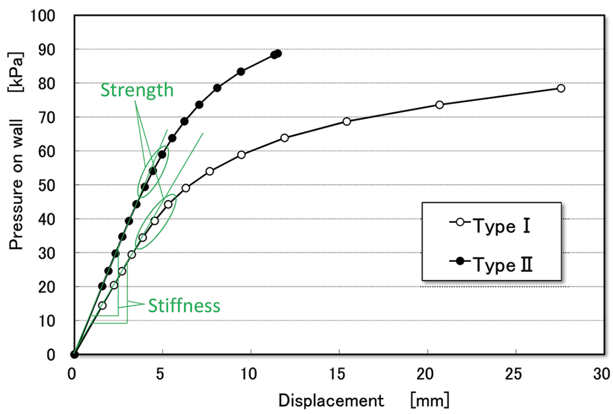

Fig. 12 Strength and stiffness of the wall

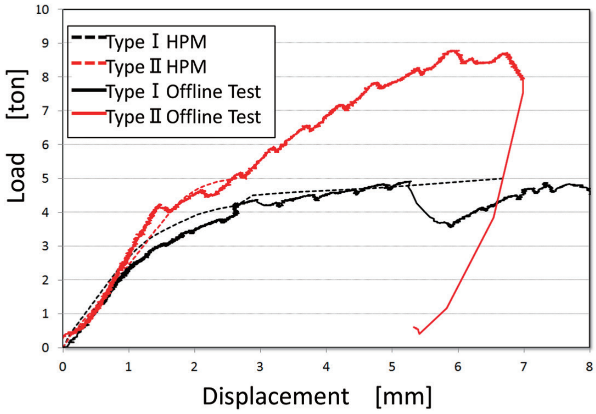

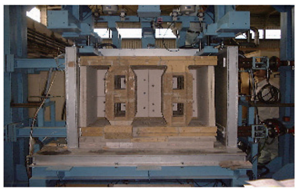

Fig. 13 Comparison with offline test and HPM analysis

displacement-load curve (shown with ○ in Fig. 12) is higher than that of Type I.

4.3.6 Comparison of unit block strength obtained by HPM analysis with offline test result

An offline fracture test was conducted using the same brick structure as that of the model used in the analysis. The values of the calculation results were higher than those of the offline test results by 20–30%. This is considered to be attributed to the local deformation (inroad) caused around the loading point (loading by a hydraulic piston). Therefore, in Type I, the effect of the inroad was eliminated and the displacement-load curve was fitted to the test curve, the result of which was used for Type II, and the prediction result is shown in **Fig. 13**. Based on this result, the calculation model is judged as valid for prediction.

4.3.7 Structural properties and its mechanism

(1) Basic block

Under this analysis condition, although there are no significant differences between the early-stage block stiffness of Type I and that of Type II, the early-stage strength of Type II is higher. This is considered to be attributed to the following: differently from Type I in which the position of the joint of the laufer section is off center, in Type II, the joint exists at the center of the laufer section, therefore, the bending moment load caused by the concentrated load at the root of the hammer brick is smaller as compared with that of Type I, while Type II is of the gate type structure wherein the concentrated load is evenly distributed in the crosswise direction, and accordingly Type II has higher yielding strength versus the concentrated load.

(2) Wall

The higher early-stage wall stiffness of Type II is considered to be attributed to the higher stiffness of its unit block and the staggered arrangement of the block in the wall which is the aggregation of the unit block.

4.4 Through crack and mechanism of generation

4.4.1 State of damage and supposable cause

Figure 14 shows the diagnosis image data of the carbonization chamber wall[32] of the coke oven at Oita Works, observed and obtained with the wall diagnosis and repair equipment. Cracks developed on the bricks between the joints of the laufer section at almost equal intervals in the furnace length direction are observable. Although not shown in the image, the cracks run through and reach the combustion chamber. Furthermore, the thermal effect is considered as the crack is generated in the entire range of the wall.

4.4.2 Objective of analysis

How the brick structure type of the coke oven affects the generation of thermal cracks and through cracks in the vertical direction is investigated. The essence of this phenomenon has already been elucidated by the analysis of a unit block using RBSM. The results thereof and of the analysis by HPM pertaining to the entire wall are introduced.

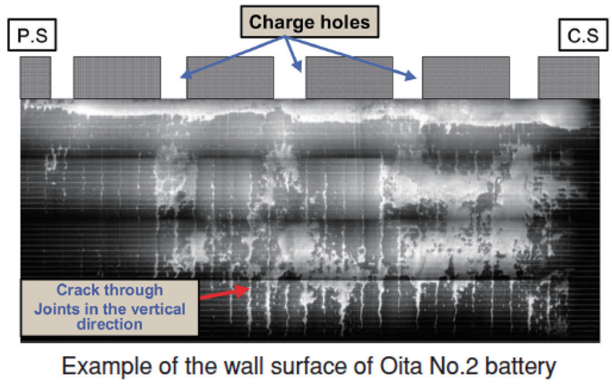

Fig. 14 Exmple of through cracks[32)]

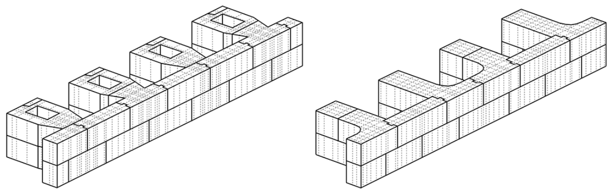

(a) Type I (b) Type II

Fig. 15 RBSM model

4.4.3 Subject of analysis and model

(1) Subject of analysis: brick structure types as shown in Fig. 6.
(2) Region of modelling: two steps of an even number step and another step of uneven number.
(3) Mesh: simplified model as shown in **Fig. 15**.
(4) Material properties: the same as those of Table 2.
(5) Heat transfer conditions: The temperature drop due to charging of coal is calculated with unsteady heat transfer analysis and the temperature distribution when the carbonization chamber surface temperature dropped to 400°C from 900°C is assumed.
(6) Loading conditions: same as Fig. 7 (a).
(7) Boundary condition: the same as Fig. 7 (a).

4.4.4 Analysis method

(1) Method: NS-Brick (RBSM)

(2) Type of analysis: Elastic analysis

(3) Type of element: Hexahedral element

4.4.5 Analysis case

In this study, analyses of the brick structures of Type I and Type II under the single level load were conducted shown in **Table 4**.

4.4.6 Analysis result

Figure 16 shows the brick temperature distribution, distribution of the longitudinal direction stress on the upper brick surface and the lower brick surface, and the distribution of the sharing stress between the upper brick and the lower brick. From this, the following facts are found.

(i) The peak of the stress emerges in the laufer section (shown with ○ in Fig. 16) and the position corresponds to the joint position of either of the upper brick or the lower brick (shown with □ in Fig. 16).

(ii) At the abovementioned stress peak position, the shearing stress between the upper brick and the lower brick reaches its peak.

4.4.7 Damage generating mechanism

In the laufer section, a jointless part and a joint part are arranged alternately in upward and downward directions, and it is considered that the joint opening developed by the repetition of the thermal shrinkage and expansion generates the peak stress on the jointless part of either of the right above brick or of the right below brick, and the crack is generated as a result thereof further promoted by the shearing stress between the upper and the lower bricks. It is considered that the once-generated crack propagates towards the combustion chamber side basically, and consequently runs through the brick and propagates in the furnace height direction in the brick.

As the number of cracks agrees with that of the joint in the laufer section, it is considered that two cracks have developed in Type I and one crack has developed in Type II.

4.4.8 State of stress on the wall obtained by HPM

Based on the abovementioned result, analysis pertaining to a model of 1/2 of the furnaces with the full height of the furnace was conducted by HPM, the model and analysis result of which are shown in **Fig. 17**. In the laufer section brick, in Type I, two straight lines of the distribution of the peak stress and the joint appearing alternately in the height-wise direction are observable, and one straight line of the same is observable in Type I.

4.5 Through hole and generating mechanism

4.5.1 State of damage and supposable cause

Figure 18 shows a typical example of through holes in a coke oven. The through hole is considered to be generated when the pressure at the time of discharging the coke acts as a concentrated load in addition to the deterioration of stiffness due to through cracks of the bricks and the deterioration of strength due to the cracks devel-

Table 4 Analysis cases

Case	Type	Region of modeling
Case-C1	Type I	2 layers × 4 bindars
Case-C2	Type II	2 layers × 4 bindars

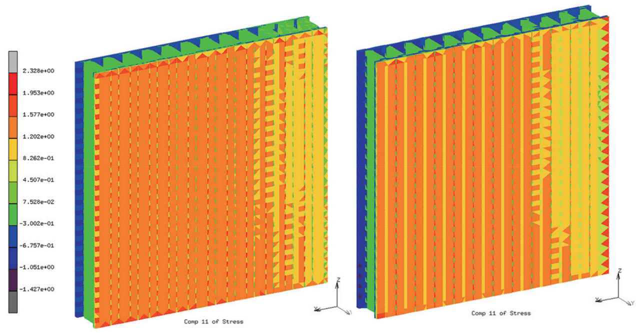

(a) Type I (b) Type II

Fig. 17 Through crack analysis using HPM

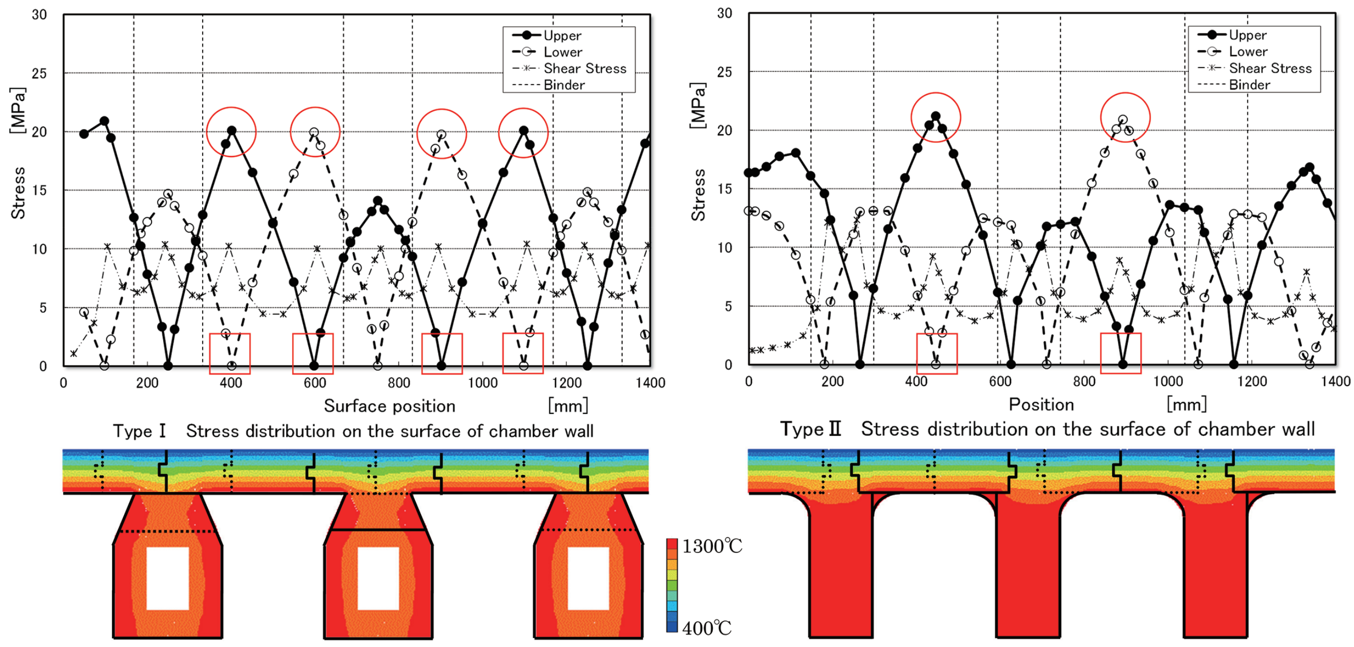

(a) Type I (b) Type II

Fig. 16 Temperature and stress distribution on bricks (—: upper, – – –: lower) oped near the dowel.

4.5.2 Objective of analysis

This analysis is intended to evaluate the possibility of the generation of the through hole due to the through crack and/or the concentrated load in a coke oven. This analysis is aimed at grasping the behavior of the wall pursuant to the mechanical concentrated load on the premise that the through cracks are generated. The influence of local thermal stress is out of scope.

4.5.3 Subject of analysis and model

(1) Subject of analysis: Type I wherein two cracks were developed.
(2) Region of modelling: 58 steps × 6 binders (symmetrical 1/2 of the entire model) and 17 steps with 4 binders (partial model).
(3) Mesh: shown in **Fig. 19**.
(4) Material properties: same as those of Table 2.
(5) Heat transfer conditions: this analysis is to evaluate the effect of the mechanical load and the temperature distribution is out of scope.
(6) Loading conditions: shown in Fig. 19, only the mechanical load influencing the through hole is given as a prerequisite.
(7) Boundary condition: shown in Fig. 19.

4.5.4 Analysis method

(1) Method: NS-Brick II (HPM)
(2) Type of analysis: Elastic analysis
(3) Type of element: Tetrahedral element

4.5.5 Analysis case

This analysis concerns Type I only, and introduces the result of the analysis when a concentrated load varying in the range from zero to fracture is applied to the center.

4.5.6 Analysis result

Figure 20 shows the deformation contour and the state of fracture when a concentrated load of 9 tons was exerted.

(i) Near the loading point in the laufer section, the displacement of the part between the joint and the crack grows large locally, and through holes are generated (Fig. 20 (c-1)).
(ii) A crack is generated in the upper laufer section of the brick and another crack is generated near the upper dowel of the lower laufer (Fig. 20 (c-2)).
(iii) Under these circumstances, the dowel of the joint remains locked, and has not yet been detached.

4.5.7 Damage generation mechanism

Two through cracks and one through crack are generated in Type I and Type II, respectively. In the case of Type I, the laufer part between the joint and the crack are restrained only by the upper and lower dowels, and is deformed greatly by the concentrated load, and considered to reach through crack ultimately along with the progress of the cracks in the laufer sections of upper and lower bricks.

Fig. 18 Example of through hole on chamber wall

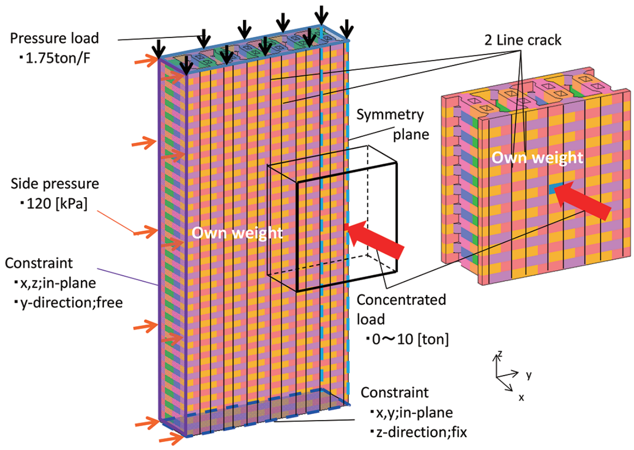

(a) Total model (b) Partial model

Fig. 19 Mesh, loading and boundary conditions

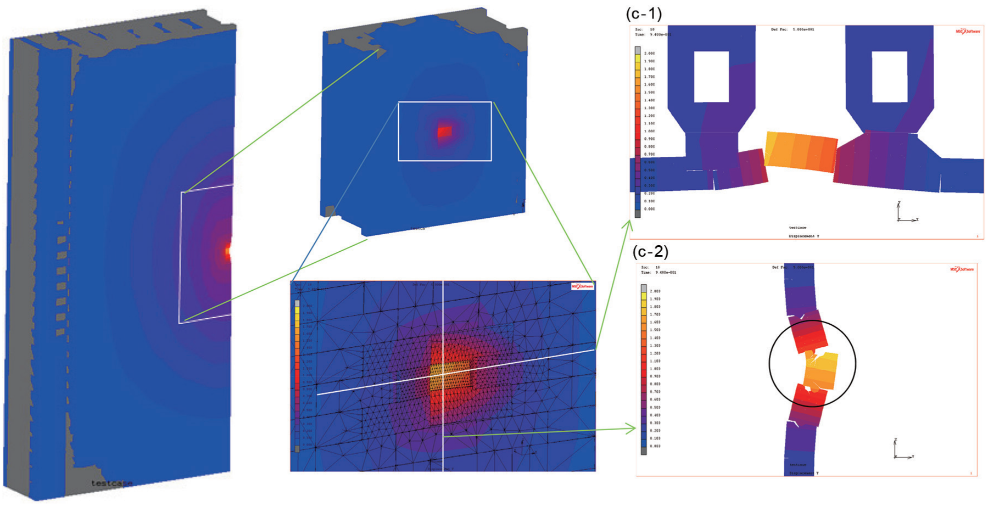

(a) Total model (b) Partial model

Fig. 20 Crack and through hole on chamber wall (magnitude: ×50)

5. Conclusion

In realizing the damage prediction for brick structures generated in operation, and the optimum design therefor, the numerical structure analysis technology plays a very important role. Because there is a limitation in applying the existing FEM to the discontinuous structure analysis, therefore, as analysis methods for discontinuum, this article has explained the flow of the efforts made in applying the limit analysis method of RBSM used for rigid body elements to the ultimate strength prediction, and the same in applying the HPM that is capable of dealing with the element deformation to the prediction of the stiffness and the strength of the brick structures, both together with their theoretical backgrounds. Furthermore, as examples of the application of these methods to actual problems, the following cases have been introduced: applications to the basic blocks of two types of coking chamber wall brick structures for the elucidation of the furnace wall stiffness and strength properties, and furthermore, to the elucidation of the generation mechanism of the through cracks and through holes.

Presently, the application of HPM is expanding to the optimization of brick properties and the brick structures for the analyses of complicated damage phenomena and for establishing countermeasures thereof, and gaining good results. Application to the problems of collapse and/or deformation of large magnitude and the development of interface with users to enhance the usability are considered to be pending subjects, and the method is to be further developed to realize such subjects.

References

1) Ngo, D., Scordelis, A.C.: Finite Element Analysis of Reinforced Concrete Beams. ACI Journal. (64-14), 152–163 (1967)
2) Goodman, E.R., Taylor, L.R., Brekke, L.T.: A Model for the Mechanics of Jointed Rock. Journal of the Soil Mechanics and Foundations Division. Proceeding of the ASCE. 1968, p. 662–685
3) Kawai, T.: New Element Models in Discrete Structural Analysis. Journal of the Society of Naval Architects of Japan. (141), 187–193 (1977)
4) Kikuchi, A., Kawai, T., Suzuki, N.: The Rigid Bodies Spring Model and Their Applications to Three-dimensional Crack Problems. Computer & Structures. 44 (1/2), 469–480 (1992)
5) Takihara, T., Uchida, H., Kikuchi, A., Toi, U.: Numerical Simulation of Nonlinear Behaviors of Three-Dimensional Block Structures. Journal of JSME. (1), 53–54 (1995)
6) Yamamura, K., Goto, K., Kikuchi, A.: Analysis of Brick Structure Using Rigid Bodies Spring Model. Refractories (Taikabutsu). 56 (9), 435–440 (2004)
7) Yamamura, K.: Applications of CAE in Solid Mechanics with a Central Focus on Discontinuous Structural Analysis. Refractories (Taikabutsu). 62 (9), 471–480 (2010)
8) Washizu, K.: Variational Methods in Elasticity and Plasticity. Pergamon Press, 1975
9) Washizu, K.: Outline of Variational Methods in Elasticity. Edited by Japanese Society of Steel Construction, Baifukan Co., Ltd, 1972 (in Japanese)
10) Takeuchi, N., Kusabuka, M., Takeda, H., Sato, K., Kawai, T.: Discrete Limit Analysis by Hybrid Type Model Using Penalty. Journal of Structural Engineering. 46A, 261–270 (2000)
11) Takeuchi, N., Ohki, H., Kanbayashi, A., Kusabuka, M.: Material Nonlinear Analysis by Using Discrete Model Applied Penalty Method in Hybrid Displacement Model. Transactions of the Japan Society for Computational Engineering and Science. 3, 53–62 (2001) (Transactions of JSCES Paper No. 20010002)
12) Yano, K., Tajiri, Y., Yamamura, K., Takeuchi, N.: On Heat Conduction and Thermal Stress Analysis by Using HPM. Proceedings of the Conference on Computational Engineering and Science. 15 (2), 513–516 (2010)
13) Ohki, H., Takeuchi, N.: Upper and Lower Bound Analysis by Hybrid-type Penalty Method. Transactions of the Japan Society for Computational Engineering and Science. 1–10 (2006) (Transactions of JSCES Paper No. 20060020)
14) Yamamura, K., Matsuzaki, S., Fuji, T., Yamada, W., Nakagawa, J.: Development of Mathematical Science in Steel Industry. Shinnittetsu Giho. (391), 143–152 (2011)
15) Kawai, T.: My Challenge in the Development of a Mixed Variational Method in Solid Mechanics. Applied Mechanics Reviews, Transaction of the ASME. (60), 51–64 (2007)
16) Cundall, P.A.: A Computer Model for Simulating Progressive, Large Scale Movements in Blocky Rock Systems. Proceedings of the Symposium of International Society of Rock Mechanics. 1, Paper No. II-1, 1971, p. 129–136
17) Shi, G.H., Goodman, R.E.: Generalization of Two-dimensional Discontinuous Deformation Analysis for Forward Modeling. International Journal for Numerical and Analytical Methods in Geomechanics. 13, 359–380 (1989)
18) Shi, G.H.: Manifold Method of Material Analysis. Trans. 9th Army Conf. on Appl. Math. and Comp. Rep. No. 92-1., U. S. Army Res. Office, 1991
19) Lucy, L. B.: A Numerical Approach to the Testing of the Fission Hypothesis. The Astronomical Journal. 82 (12), 1013–1024 (1977)
20) Koshizuka, S., Oka, Y.: Moving-Particle Semi-implicit Method for Fragmentation of Incompressible Fluid. Nucl. Sci. Eng. (123), 421–434 (1996)
21) Libersky, L.D., Petschek, A.G., Carney, T.C., Hipp, J.R., Allahdadi, F.A.: High Strain Lagrangian Hydrodynamics—A Three-Dimensional SPH Code for Dynamic Material Response—. J. Comput. Phys. (109), 67–75 (1993)
22) Koshizuka, S., Chikazawa, Y., Oka, Y.: Particle Method for Fluid and Solid Dynamics. Computational Fluid and Solid Mechanics. (2), 1269–1271 (2001)
23) Onate, E., Idelsohn, S.R., Celigueta, M.A., Rossi, R.: Advances in the Particle Finite Element Method for the Analysis of Fluidmultibody Interaction and Bed Erosion in Free Surface Flows. Computer Methods in Applied Mechanics and Engineering. 197, 1777–1800 (2008)
24) Takeuchi, N., Tajiri, Y., Yamamura, K.: On Estimation for Stress in Element of Rigid Bodies-Spring Model. Study Report of Research Center for Computing and Multimedia Studies, Hosei University. 22, 7–14 (2009)
25) Tajiri, Y., Yamamura, K., Takeuchi, N.: Evaluation of Stress in Element of RBSM using Principle of Hybrid-type Virtual Work. Proceedings of the Conference on Computational Engineering and Science. 14 (2), 691–694 (2009)
26) Tajiri, Y., Yamamura, K., Takeuchi, N.: Development of Modified RBSM by Principle of Hybrid-type Virtual Work. Journal of Structural Engineering. 56A, 169–178 (2010)
27) Kurita, M., Tajiri, Y., Yamamura, K., Takeuchi, N.: Discrete Limit Analysis with Modified RBSM. Proceedings of the Conference on Computational Engineering and Science. 15 (2), 501–504 (2010)
28) Yamada, Y., Yoshimura, N., Sakurai, T.: Plastic Stress-strain Matrix and Its Application for the Solution of Elastic-plastic Problems by Finite Element Method. Int. J. Mechanical Science. 10, 323–354 (1968)
29) Takeuchi, N.: Discrete Limit Analysis in Geomechanics. Baifukan Co., Ltd, 1991 (in Japanese)
30) Sakaida, M., Awa, Y., Sugiura, M., Nakajima, J., et al. : Development of Diagnosis / Repair Apparatus for Coke Oven Chamber Wall. Shinnittetsu Giho. (384), 63–68 (2006)
31) Kasai, K., Tsutsui, Y.: Recent Technology of Coke Oven Refractories. Shinnittetsu Giho. (388), 54–61 (2008)
32) Kobayashi, S., Nakajima, J.: Development of Repair Apparatus for Coking Chamber Walls on Coke Oven. Shinnittetsu Giho. (402), 45–50 (2015)

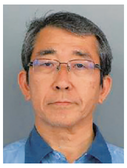
Kazuto YAMAMURA
Chief Researcher
Process Technology Div.
Process Research Laboratories
20-1 Shintomi, Futtsu City, Chiba Pref. 293-8511


Norio TAKEUCHI
Professor, Dr.Eng.
Department of Engineering and Design
Faculty of Engineering and Design
Hosei University


Yasuyuki TAJIRI
Manager, Dr.Eng.
CAE Dept. TAC Center, Yawata Unit
Nippon Steel & Sumikin Technology Co., Ltd.